Monthly Notices of the ROYAL ASTRONOMICAL SOCIETY

MNRAS **523,** L58–L63 (2023) https://doi.org/10.1093/mnrasl/slad059
Advance Access publication 2023 May 18

GlobULeS – V. UVIT/*AstroSat* studies of stellar populations in NGC 362: detection of blue lurkers in a globular cluster

Arvind K. Dattatrey [1,2★] R. K. S. Yadav,[1] Gourav Kumawat,[3] Sharmila Rani,[4] Gaurav Singh,[4] Annapurni Subramaniam[4] and Ravi S. Singh[2]

[1]*Aryabhatta Research Institute of Observational Sciences, Manora Peak, Nainital 263001, Uttarakhand, India*
[2]*Deen Dayal Upadhyay Gorakhpur University, Gorakhpur 273009, Uttar Pradesh, India*
[3]*Indian Institute of Science Education and Research, Bhopal 462066, Madhya Pradesh, India*
[4]*Indian Institute of Astrophysics, Koramangala, Bangalore 560034, Karnataka, India*

Accepted 2023 May 12. Received 2023 May 6; in original form 2023 March 7

ABSTRACT

We report the discovery of four blue lurkers with low- and extremely low mass white dwarf (ELM WD) companions in the Galactic globular cluster NGC 362 using *AstroSat*'s Ultra Violet Imaging Telescope (UVIT). We analysed the multiwavelength spectral energy distribution (SED) of far-ultraviolet-bright main-sequence stars using data from the UVIT, Ultraviolet Optical Telescope, *Gaia* EDR3, and 2.2-m ESO/MPI telescopes. Two each of low-mass WDs and ELM WDs are found as companions for the four blue lurkers by the fitting of two-component SED models. The effective temperatures, radii, luminosities, and masses of two low-mass WDs are (35 000, 23 000) K, (0.04, 0.05) $R_{\odot}$, (1.45, 0.22) $L_{\odot}$, and (0.2, 0.2) $M_{\odot}$, while the two ELM WDs are (14 750, 14 750) K, (0.09, 0.10) $R_{\odot}$, (0.34, 0.40) $L_{\odot}$, and (0.18, 0.18) $M_{\odot}$, respectively. The position of blue lurkers within the cluster shows that they originated via the Case A/B mass-transfer mechanism in a low-density environment. This is the first detection of blue lurkers with low-mass WDs and ELM WDs as companions in a globular cluster. The companion's cooling age is less than 4 Myr, which suggests that they were just recently formed. These binary systems might have originated due to the cluster's recent core collapse.

Key words: ultraviolet: stars – blue lurkers – Hertzsprung–Russell and CM diagrams – white dwarfs – Globular star clusters: individual: NGC362.

1 INTRODUCTION

Sandage (1953) discovered stars brighter and bluer than the main sequence lying above the turn-off in the colour–magnitude diagram (CMD) of the Galactic globular cluster (GGC) M3. These stars are called Blue Straggler Stars (BSSs). The three major formation pathways for BSSs are as follows: mass transfer (MT) in binary star systems via Roche lobe overflow (RLOF), which leads to mass gain by BSS progenitors (McCrea 1964); stellar collisions in a dense cluster environment (Hills & Day 1976); and tightening and merger of inner binaries in a hierarchical triple system (Perets & Fabrycky 2009; Naoz & Fabrycky 2014).

Blue lurkers (BLs), like BSSs, are also post-MT systems, but they do not appear brighter than the main-sequence turn-off (MSTO) in the CMD. This could be due to a lack of accreted matter or a too-small accretor star. The jump in the CMD for these stars is insufficient for them to be seen above the MSTO. As a result, these stars have been designated as BLs: 'BSS-type stars lying hidden in the MS below MSTO' (Leiner et al. 2019). These stars cannot be detected using the CMD alone because they do not stand out like BSSs. Some possible techniques to find these stars are as follows: observation of more than average rotation (Vsini) indicating a recent MT event (Leiner et al. 2019); multiwavelength spectral energy distribution (SED) analysis to find companions such as extremely low mass (ELM) white dwarfs (WDs), hot sub-dwarfs, etc. (Jadhav, Sindhu & Subramaniam 2019; Subramaniam et al. 2020); and looking for chemical peculiarities possible only via mass accretion. In fact, *N*-body simulations and population synthesis studies predict that such MT products could be abundant (Andronov, Pinsonneault & Terndrup 2006; Geller, Hurley & Mathieu 2013).

ELM WDs are helium-core WDs with masses $M \leq 0.18$ $M_{\odot}$ (Sun & Arras 2018). The Universe's age limits the mass of WDs formed by isolated star evolution to $\approx$0.4 $M_{\odot}$ (Brown et al. 2010). WDs with masses 0.1–0.4 $M_{\odot}$ were found to be part of compact binaries (Marsh, Dhillon & Duck 1995; Benvenuto & De Vito 2004; Brown et al. 2010). Their formation can be explained by mass-loss in binary systems.

Relatively few studies have been done to identify BLs, only in open clusters (OCs; Jadhav et al. 2019; Leiner et al. 2019; Subramaniam et al. 2020). These BLs are found in binary systems with WD/low-mass WD companions. To our knowledge, no literature exists on the detection of BLs in GCs. Here, we report the first detection of BLs in the GC NGC 362 using ultraviolet (UV) data.

The GC NGC 362 is located in the Tucana constellation in the Southern hemisphere (RA = $01^{h}\,03^{m}\,14\overset{s}{.}26$ and Dec. = $-70^{\circ}\,50'\,55\overset{''}{.}6$). The cluster has an age of $\approx$11 Gyr, located at

★ E-mail: arvind@aries.res.in

a distance of ≈8.83 kpc (Vasiliev & Baumgardt 2021), a metallicity $[Fe/H]$ of ≈−1.3 dex, and a reddening of ∼0.05 mag (Harris 2010).

2 DATA SETS AND THEIR REDUCTION

The observations of NGC 362 were made with the Ultra Violet Imaging Telescope (UVIT) on 2016 November 11, in four UV filters: *F*148*W*, *F*169*M*, *N*245*M*, and *N*263*M*. UVIT is one of the payloads on *AstroSat*, India's first multiwavelength space observatory, which was launched on 2015 September 28. The exposure times were 4900, 4600, 4900, and 4600 s in the *F*148*W*, *F*169*M*, *N*245*M*, and *N*263*M* filters, respectively. Using the CCDLAB software (Postma & Leahy 2017), which corrects for satellite drift, flat-field, geometric distortion, fixed pattern noise, and cosmic rays, data reduction of the raw images was carried out. Detailed descriptions of the telescope, instruments, and preliminary calibration can be found in Subramaniam et al. (2016b) and Tandon et al. (2017).

The archival UV data collected with Ultraviolet Optical Telescope (UVOT) are also used in this analysis. The raw data from the HEASARC archive[1] was processed using the HEA-Soft[2] pipeline. The telescope's details and photometric calibration of UVOT data can be found in Poole et al. (2008). Corrections were made to exposure maps and auxiliary spacecraft data, as well as to science images that were geometrically corrected for sky coordinates. In order to process the UVOT/*Swift* data, the procedure outlined by Siegel et al. (2014) was used. In addition, archival optical data in the *U*, *B*, *V*, *R*, and *I* filters collected by the Wide-Field Imager mounted on the 2.2-m ESO/MPI Telescope were utilized. The details of data reduction and photometry are provided in Anderson et al. (2006).

3 UV AND OPTICAL COLOUR–MAGNITUDE DIAGRAMS

3.1 The selection of FUV-bright stars on the main sequence

Before identifying the far-ultraviolet (FUV)-bright MS stars, we cross-matched the UVIT data with the *Gaia* EDR3 photometric data with a matching radius of 1.0 arcsec. The FUV-bright MS stars are selected using the UV–optical CMDs. We utilized the proper-motion membership probability catalogue from the GlobULeS I paper (Sahu et al. 2022) to select the members. The membership probabilities are based on the *Gaia* DR3 proper motions and a comprehensive comparison of the cluster-like stars' kinematics distribution and the field distribution. Stars with a membership probability greater than 85 per cent were chosen as cluster members and considered for further analysis. We constructed the UV–optical CMDs of members by finding the optical counterparts of the UVIT-detected sources.

We plotted the FUV–optical CMD [*F*148*W*, (*F*148*W* − *G*)] of BSSs shown in the left-hand panel of Fig. 1. The dotted and solid lines represent the ZAMS and MS curves taken from BaSTI.[3] The BSS (blue symbols) sequence is easily identified in the CMD. Four FUV-bright stars (ID: 1551, 1991, 2412, and 2481) can be found bluer than the ZAMS. To check the location of these four FUV-bright stars in the optical CMD, we constructed [*G*, ($G_{BP} - G_{RP}$)] diagram shown in the middle panel of Fig. 1. For visual guidance, we overplotted BaSTI isochrone with a solid line using the cluster's parameters given in Section 1. It is evident that the four FUV-bright stars are located close to the turn-off point of the cluster in the optical CMD. We analysed the locations and contamination of these stars in the observed image and marked them with red squares in the *F*148*W* image, as depicted in the right-hand panel of Fig. 1. This figure reveals that the stars are clearly resolved, with no contamination. They are situated more than 3 arcmin from the cluster's centre.

4 SPECTRAL ENERGY DISTRIBUTIONS

In this section, we build the SED of the FUV-bright MS stars 1551, 1991, 2412, and 2481 to look for the companions and their properties. We used the virtual observatory tool, VOSA (VO SED Analyzer; Bayo et al. 2008) for this. VOSA uses filter transmission curves to compute synthetic photometry for a chosen theoretical model. The synthetic photometric data are then compared to the observed data, and the best fit is determined using the χ^2 minimization test. The specific procedures for single and binary component SED fitting are provided in Subramaniam et al. (2016a) and Rani et al. (2021).

In brief, we fit the model of Castelli & Kurucz (2003) of varying temperature and surface gravity with a fixed metallicity of $[Fe/H] = -1$ dex using the basic parameters provided in Section 1. The effective temperatures were considered to be in the 5000–50 000 K range, with log *g* ranging from 3 to 5 dex. The UVIT data were combined with UVOT and ESO 2.2-m optical data for long coverage of wavelengths in the SED.

We used the Kurucz stellar atmospheric model to fit the single-component SED, as shown with a grey curve in Fig. 2. The observed data are represented by red points with error bars, whereas the model data are represented by blue points. The residuals between the fitted model and the observed fluxes, normalized by the observed flux, are shown in the bottom panel of each SED. The green points, along with the error bars, are the residuals, and the dashed horizontal lines at ±0.3 (30 per cent) are the residual threshold. The residual plots in Fig. 2 show that the residual flux in the UV region is greater than 0.3 in more than one data point. This indicates a UV excess in all four FUV-bright MS stars, and a combination of hotter and cooler spectra may fit the SEDs.

We fitted two-component SEDs to account for the UV excess. We used the Kurucz stellar atmospheric model (Castelli, Gratton & Kurucz 1997; Castelli & Kurucz 2003) to fit the cooler component and the Koester WD model (Koester 2010) (shown with cyan curves) to fit the hotter component. $T_{\rm eff}$ and log *g* in the Koester WD model range from 5000–80 000 K and 6.5–9.5, respectively. The combined spectra are shown with a black line in Fig. 2. The fitting parameters χ^2_r, $V_{\rm gf}$, and $V_{\rm gfb}$ of the combined spectra, listed in Table 1, indicate that the spectrum fits well for all wavelengths. The Koester model fits the hot components well, while the Kurucz model fits the cool components well. The fractional residuals for the combined SEDs are shown as black points along with the error in the bottom panels. For the combined SEDs, the residuals are within 0.3 on each wavelength.

Fitting the two components yields the fundamental parameters of the cool and hot components of the FUV-bright MS stars. The estimated parameters are shown in Table 1. The star IDs with 'A' and 'B' represent the cool and hot components, respectively. The range of parameters for cool components is $T_{\rm eff} \sim$ 6250–6750 K, log *g* ∼ 3–5, $L \sim$ 1.02–3.21 $L_\odot$, and $R \sim$ 0.90–1.53 $R_\odot$, while those for hot components are $T_{\rm eff} \sim$ 14 750–35 000 K, log *g* ∼ 6.5–9.5, $L \sim$ 0.22–1.45 $L_\odot$, and $R \sim$ 0.04–0.10 $R_\odot$.

The effective temperature and radius of 11 BLs found in the OC M67 have been calculated by Leiner et al. (2019) using SED analysis. The effective temperature and radius were found to be in the 5520–

[1] https://heasarc.gsfc.nasa.gov
[2] https://heasarc.gsfc.nasa.gov/docs/software/heasoft
[3] http://basti-iac.oa-abruzzo.inaf.it/

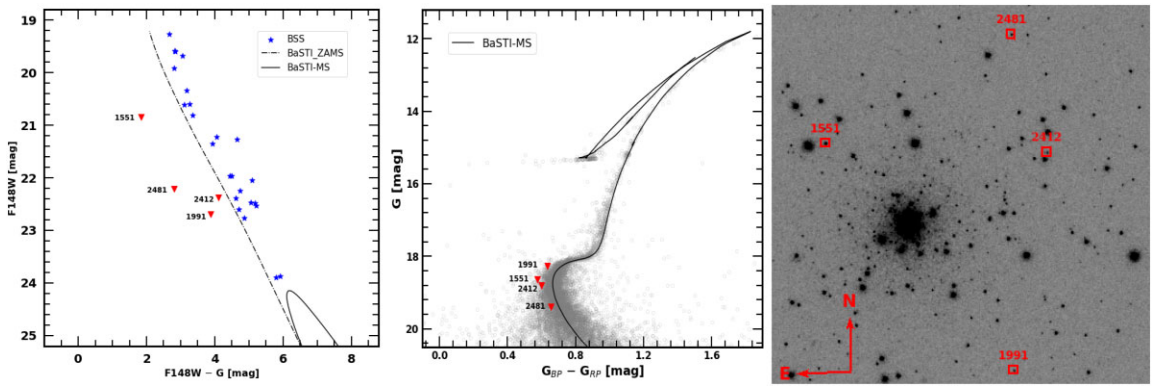

Figure 1. Left-hand panel: UV–optical CMD ($F148W$ versus $F148W - G$) of the BSSs for the cluster NGC 362. Blue symbols represent the BSSs. The probable four BL candidates, bluer than the ZAMS, are displayed with red down-triangle symbols. Middle panel: The optical CMD (G versus $G_{BP} - G_{RP}$) of the cluster NGC 362. The BaSTI isochrone is overplotted with a solid black line. The four red down-triangle symbols represent the FUV-bright MS stars. Right-hand panel: Spatial locations of the four FUV-bright MS stars in $F148W$ image of NGC 362. The field of view of the image is ∼8.5 arcmin × 8.5 arcmin. North is up and east is on the left.

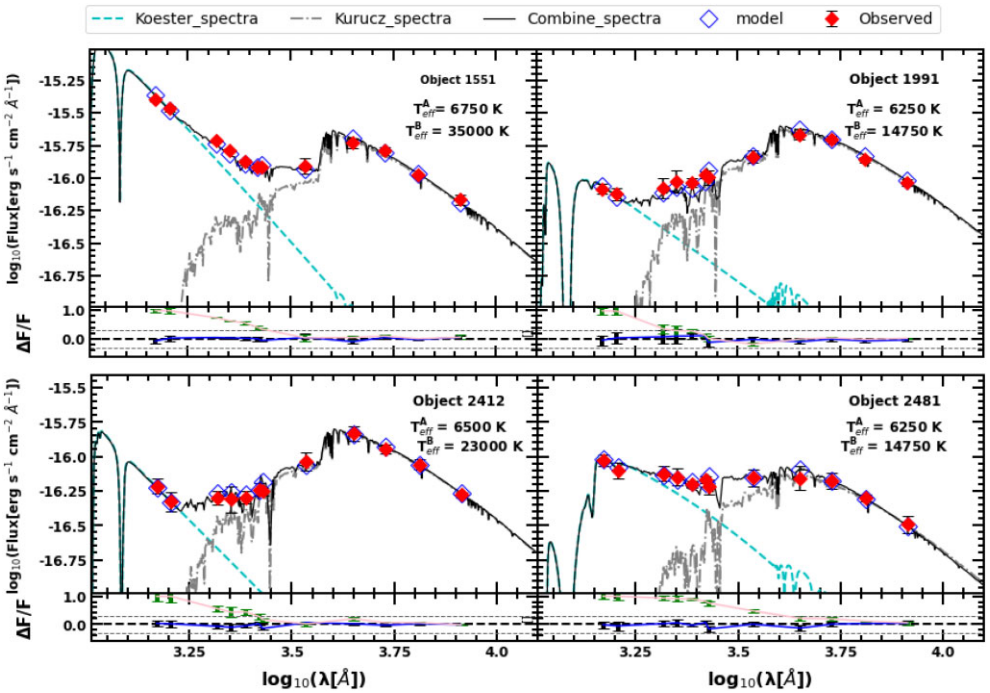

Figure 2. The SEDs of four FUV-bright MS stars (1551, 1991, 2412, and 2481). $T_{\rm eff}$ of the cool (A) and hot (B) components are displayed in each SED. The observed data points are represented by red solid diamond points, while open blue diamond points represent the model points. Cyan, grey, and black curves represent the Koester, Kurucz, and combined spectra, respectively. $\Delta F/F$ is the fractional residual.

6840 K and 0.85–1.9 $R_\odot$ ranges, respectively. The present estimated parameters for the BLs are well within the range.

4.1 Age and mass of the cool and hot components

We estimated the age and mass of the cool components, 1551A, 1991A, 2412A, and 2481A, by comparing their positions to theoretical isochrones retrieved from BaSTI (Pietrinferni et al. 2021) in the HR diagram shown in Fig. 3. We considered the SED-estimated surface temperature and luminosity of cool components, which are represented by red points in the figure. The isochrones from 5 to 11 Gyr are plotted with intervals of 0.5 Gyr using grey lines with the cluster's input parameters provided in Section 1. By comparing the positions to the isochrones, the cool components 1551A, 1991A, 2412A, and 2481A have ages of 5.5, 10, 8, and 5.5 Gyr and masses of 0.92, 0.85, 0.87, and 0.82 $M_\odot$, respectively. The estimated age and mass of each cool component are displayed in Table 1.

The age and mass of 1551B, 1991B, 2412B, and 2481B (hot components) are derived using the HR diagram depicted in Fig. 3. The surface temperature and luminosity derived using SEDs are used in the HR diagram. Cyan points denote the hot components. A blue and yellow line represents a 0.2 and 0.3 $M_\odot$ helium DB WD models from Tremblay & Bergeron (2009). The ELM WD models of mass 0.182 and 0.186 $M_\odot$ are shown with magenta lines, which were taken from Althaus, Miller Bertolami & Córsico (2013). The two hot components, 1991B and 2481B, are located on the 0.186 $M_\odot$ ELM

Table 1. The best-fitting parameters of the cool and hot components. Here, $T_{\rm eff}$ is the effective temperature in K, χ^2_r is reduced χ^2, luminosity, radius, and mass are in the solar unit, $V_{\rm gf}$ and $V_{\rm gfb}$ are the visual goodness of fit parameters, and $N_{\rm fit}$ is the total number of points taken into account during the fitting. The mass and age of cool and hot companions are listed in the last two columns.

Name	RA	Dec.	$T_{\rm eff}$ (K)	Log g	χ^2_r	$L/L_\odot$	$R/R_\odot$	$V_{\rm gf}$	$V_{\rm gfb}$	$N_{\rm fit}$	Mass ($M_\odot$)	Age (Myr)
1551A	15.893 96	−70.819 36	6750^{+125}_{-125}	3.0	58.76	$2.45^{+0.009}_{-0.300}$	$1.15^{+0.005}_{-0.002}$	29.8	1.37	12/12	0.92	5500
1551B			$35\,000^{+3000}_{-1000}$	9.5		$1.45^{+0.292}_{-0.170}$	$0.04^{+0.003}_{-0.005}$				0.2	<0.10
1991A	15.699 60	−70.900 77	6250^{+125}_{-125}	3.5	6.07	$3.21^{+0.181}_{-0.020}$	$1.53^{+0.001}_{-0.003}$	4.68	0.21	12/12	0.85	10 000
1991B			$14\,750^{+250}_{-500}$	7.0		$0.34^{+0.0134}_{-0.010}$	$0.09^{+0.008}_{-0.003}$				0.18	∼4.0
2412A	15.657 96	−70.824 86	6500^{+125}_{-125}	3.5	4.39	$1.99^{+0.294}_{-0.121}$	$1.18^{+0.001}_{-0.002}$	4.37	0.88	12/12	0.87	8000
2412B			$23\,000^{+500}_{-1000}$	6.5		$0.22^{+0.011}_{-0.003}$	$0.05^{+0.005}_{-0.002}$				0.2	<0.10
2481A	15.692 60	−70.783 16	6250^{+125}_{-125}	5.0	15.25	$1.02^{+0.270}_{-0.080}$	$0.90^{+0.015}_{-0.015}$	10.70	2.92	12/12	0.82	5500
2481B			$14\,750^{+250}_{-750}$	9.5		$0.40^{+0.085}_{-0.001}$	$0.10^{+0.013}_{-0.001}$				0.18	∼4.0

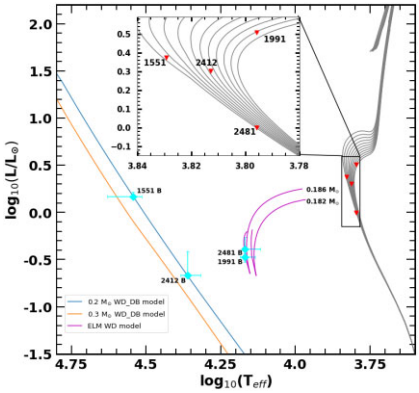

Figure 3. The HR diagram of the cool and hot components. Red and cyan points, respectively, represent the cool and hot components. The grey, sky blue, and magenta curves represent the BaSTI isochrones, the WD model, and the ELM models, respectively. The WD model is for 0.2 $M_\odot$, while the ELM model is for 0.182 and 0.186 $M_\odot$.

WD model, while 1951B and 2412B are very close to the 0.2 $M_\odot$ WD DB model. The models predict cooling ages of ≤0.1 Myr for 1551B and 2412B and 4 Myr for 1991B and 2481B. The mass and cooling age of the hot components are listed in Table 1.

5 RESULTS AND DISCUSSION

Using the UVIT, UVOT, and 2.2-m ESO optical data, we discovered four FUV-bright MS stars in the GGC NGC 362. We built the SEDs using VOSA to determine their physical characteristics and identify any companions that might be present. The fitting of single-component SED to the observed data points reveals the UV excess in all four stars. To account for the UV excess, we fitted the SED of two components. The combined spectra of cool and hot components fit well to all four stars. This study indicates that these stars are in binary systems.

Based on the current analysis of the SEDs of four FUV-bright MS stars, the surface temperature, luminosity, radius, mass, and age of the cool components 1551A, 1991A, 2412A, and 2481A are determined to be in the range of 6250–6750 K, 1.02–3.21 $L_\odot$, 0.90–1.53 $R_\odot$, 0.82–0.92 $M_\odot$, and 5.5–10 Gyr, respectively. The masses of these components are near the cluster's turn-off mass (0.8 $M_\odot$). In comparison to the BSSs, their positions on the HR diagram are close to the cluster's turn-off point. The derived age of the cool components reveals that they are younger than the cluster (11 Gyr). The present analysis leads us to believe that these cool components could be BLs. They have been regenerated by MT like the BSSs but mixed with the normal MS population in the CMD. As the cluster ages, similar-mass stars will evolve away from the MS, showing these lurkers as BSSs (Leiner et al. 2019).

The surface temperatures, luminosities, and radii of the hot components 1551B, 1991B, 2412B, and 2481B were found to range from 14 750–35 000 K, 0.22–1.45 $L_\odot$, and 0.04–0.1 $R_\odot$, respectively, based on the best SED fits.

The mass and cooling age of 1551B and 2412B are 0.20 $M_\odot$ and ≤0.1 Myr, respectively, while those of 2481B and 1991B are 0.186 $M_\odot$ and 4 Myr, respectively. Based on the estimated parameters, locations, and superimposed models in the HR diagram, we can deduce that 1551B and 2412B are low-mass helium-core WDs, while 2481B and 1991B are ELM WDs.

We found that the newly discovered FUV-bright MS stars are binary systems. The stars 1551 and 2412 have a pair of BL + low-mass WDs, whereas 2481 and 1991 have a pair of BL + ELM WDs. Because BLs are a smaller mass group of BSSs, the formation mechanism may be similar to that of the BSSs. Similar to BSSs, these are post-MT systems. The masses of hot companions are found to be 0.186 and 0.2 $M_\odot$. It is unlikely that such low-mass WD candidates will form through a single, isolated star evolution. They might have originated in binary systems. The mass of WDs created by a single star evolution is restricted to 0.4 $M_\odot$ (Brown et al. 2010). The age of the universe limits the lower end of the WD mass range. However, ELM WDs can be found in binaries (Jadhav et al. 2019; Ratzloff et al. 2019; Subramaniam et al. 2020; Vaidya et al. 2022; Dattatrey et al. 2023). Mass-loss in the early phases of evolution sets a minimum value for WD masses. It is possible that the case A/B MT will lead to the He-core WDs through early envelope mass-loss (Iben 1991; Marsh et al. 1995). As a result, MT is required for the creation of low-mass WDs in tight binary systems where the companion tears away the low-mass WD progenitor's envelope and the low-mass core fails to ignite the He core. The companion star acquired mass and evolved into BLs during the mass-loss. Li et al. (2019) claim that ELM WDs with masses less than 0.22 $M_\odot$ are generated through the RLOF channel. This leads us to the further conclusion that these BLs are produced via MT with a WD companion.

The formation of investigated binary systems may be related to the dynamical evolution of the cluster. The cooling ages of low-mass WDs and ELM WDs are <0.1 and 4 Myr, respectively. Dalessandro et al. (2013) suggest that NGC 362 is either experiencing or about to

experience the core collapse based on the density profile. The cooling ages of the hot companions show that they have only recently formed. As a result, we might infer that these binary systems might have originated during the cluster's core collapse. During the collapse, the centre density grows quickly, increasing the chances of gravitational interactions as well (Meylan & Heggie 1997) as the creation of binary systems that are brought into the MT regime by hardening processes caused by gravitational encounters (McMillan, Hut & Makino 1990; Hurley et al. 2008). On the other hand, based on the radial distribution of BSS, Dalessandro et al. (2013) found that the core collapse may have begun around 200 Myr ago, which is significantly earlier than the expected formation epoch of BLs. Therefore, presuming that cluster properties can play a role in the formation of BLs, it is more probable that they formed during the post-core-collapse rebounce phases.

The four BLs are located more than 3 arcmin from the cluster centre. The origin of these BLs in the cluster's outskirts is unknown. We speculate that these BLs, like BSS, may have been created by collisions during resonance encounters between binary and single stars in the core and ejected into the outer regions by the recoil from the interactions (Bolte, Hesser & Stetson 1993; Sigurdsson, Davies & Bolte 1994). The discovery of BLs + WDs systems in the outer area of the near-core-collapse cluster has consequences for GCs' dynamical evolution theories. The total census of BLs on cluster MSs is mainly unknown because of the difficulty of discovering them. The stellar characteristics of this vital population are, as a result, poorly understood.

Another possibility for the origin of these BLs is the MT in the primordial close binary systems located in the outer region of the cluster. According to Dalessandro et al. (2013), NGC 362 is a dynamically old cluster, which means that even the external BSSs have sunk towards the cluster's centre due to the mass segregation process. As BLs have low mass compared to BSSs, the impact of mass segregation on BLs will be smaller than that on BSSs. As a result, they are still in the cluster's outer region.

The BLs are located in the outer part of the cluster, which makes them an intriguing spectroscopic study target. The spectroscopy can provide an accurate estimation of the parameters and their nature to constrain their formation paths.

Due to the low spatial resolution, we do not explore the BLs at the cluster's centre. To get a complete sample of BLs, we need high-resolution and deeper UV observations.

6 SUMMARY AND CONCLUSIONS

The first detection of BLs in the GGC NGC 362 is presented. This result is based on observations from *AstroSat* UVIT as well as archival data from UVOT and the 2.2-m ESO/MPI telescopes. We can draw the following conclusions from this study:

(i) We found four FUV-bright MS stars in cluster NGC 362. The SED study reveals an excess in FUV flux from all four sources. To account for the FUV excess, we fitted a two-component SED model.

(ii) The cool companions are fitted with the Kurucz model, and the hot companions are fitted with the Koester model. The parameters obtained from the two-component SED model are shown in Table 1. Based on our SED analysis, we conclude that the cool companions of all four sources are BLs. The hot companions of 1551 and 2412 are low-mass helium-core WDs, whereas 2481 and 1991 are ELM WDs.

(iii) The location of these four sources within the cluster suggests that they were formed via the Case A/B MT process. The cluster is currently undergoing a core collapse. The cooling age of hot companions indicates that they were generated very recently. We suggest that these binary systems were formed during the core-collapse process and were ejected from the core due to gravitational interaction.

ACKNOWLEDGEMENTS

We warmly thank Pierre Bergeron for providing us with the WD cooling models generated for UVIT filters. I would like to thank Dr Sindhu Pandey for her help with UVIT data reduction. I want to thank Gurpreet Singh for his assistance during this project. AS thanks the support of the Science and Engineering Research Board (SERB) power fellowship. This paper is based on observations collected at the European Organization for Astronomical Research in the Southern hemisphere under ESO programme 60.A-9121(A).

DATA AVAILABILITY

The data utilized in this article will be provided upon request.

REFERENCES

Althaus L. G., Miller Bertolami M. M., Córsico A. H., 2013, A&A, 557, A19
Anderson J., Bedin L. R., Piotto G., Yadav R. S., Bellini A., 2006, A&A, 454, 1029
Andronov N., Pinsonneault M. H., Terndrup D. M., 2006, ApJ, 646, 1160
Bayo A., Rodrigo C., Barrado Y Navascués D., Solano E., Gutiérrez R., Morales-Calderón M., Allard F., 2008, A&A, 492, 277
Benvenuto O. G., De Vito M. A., 2004, MNRAS, 352, 249
Bolte M., Hesser J. E., Stetson P. B., 1993, ApJ, 408, L89
Brown W. R., Kilic M., Allende Prieto C., Kenyon S. J., 2010, ApJ, 723, 1072
Castelli F., Kurucz R. L., 2003, in Piskunov N., Weiss W. W., Gray D. F., eds, Proc. IAU Symp. 210, Modelling of Stellar Atmospheres, Poster Contributions. Kluwer, Dordrecht, p. A20
Castelli F., Gratton R. G., Kurucz R. L., 1997, A&A, 318, 841
Dalessandro E. et al., 2013, ApJ, 778, 135
Dattatrey A. K., Yadav R. K. S., Rani S., Subramaniam A., Singh G., Sahu S., Singh R. S., 2023, ApJ, 943, 130
Geller A. M., Hurley J. R., Mathieu R. D., 2013, AJ, 145, 8
Harris W. E., 2010, preprint (arXiv:1012.3224)
Hills J. G., Day C. A., 1976, Astrophys. Lett., 17, 87
Hurley J. R. et al., 2008, AJ, 135, 2129
Iben Icko. J., 1991, ApJS, 76, 55
Jadhav V. V., Sindhu N., Subramaniam A., 2019, ApJ, 886, 13
Koester D., 2010, Mem. Soc. Astron. Ital., 81, 921
Leiner E., Mathieu R. D., Vanderburg A., Gosnell N. M., Smith J. C., 2019, ApJ, 881, 47
Li Z., Chen X., Chen H.-L., Han Z., 2019, ApJ, 871, 148
McCrea W. H., 1964, MNRAS, 128, 147
McMillan S., Hut P., Makino J., 1990, ApJ, 362, 522
Marsh T. R., Dhillon V. S., Duck S. R., 1995, MNRAS, 275, 828
Meylan G., Heggie D. C., 1997, A&AR, 8, 1
Naoz S., Fabrycky D. C., 2014, ApJ, 793, 137
Perets H. B., Fabrycky D. C., 2009, ApJ, 697, 1048
Pietrinferni A. et al., 2021, ApJ, 908, 102
Poole T. S. et al., 2008, MNRAS, 383, 627
Postma J. E., Leahy D., 2017, PASP, 129, 115002
Rani S., Pandey G., Subramaniam A., Sahu S., Rao N. K., 2021, MNRAS, 501, 2140
Ratzloff J. K. et al., 2019, ApJ, 883, 51
Sahu S. et al., 2022, MNRAS, 514, 1122
Sandage A. R., 1953, AJ, 58, 61
Siegel M. H. et al., 2014, AJ, 148, 131
Sigurdsson S., Davies M. B., Bolte M., 1994, ApJ, 431, L115

Subramaniam A. et al., 2016a, ApJ, 833, L27
Subramaniam A. et al., 2016b, in den Herder J.-W. A., Takahashi T., Bautz M., eds, Proc. SPIE Conf. Ser. Vol. 9905, Space Telescopes and Instrumentation 2016: Ultraviolet to Gamma Ray. SPIE, Bellingham, p. 99051F
Subramaniam A., Pandey S., Jadhav V. V., Sahu S., 2020, J. Astrophys. Astron., 41, 45
Sun M., Arras P., 2018, ApJ, 858, 14
Tandon S. N. et al., 2017, AJ, 154, 128
Tremblay P. E., Bergeron P., 2009, ApJ, 696, 1755
Vaidya K., Panthi A., Agarwal M., Pandey S., Rao K. K., Jadhav V., Subramaniam A., 2022, MNRAS, 511, 2274
Vasiliev E., Baumgardt H., 2021, MNRAS, 505, 5978

This paper has been typeset from a TEX/LATEX file prepared by the author.